Primary mouse hepatocytes for systems biology approaches: a standardized *in vitro* system for modelling of signal transduction pathways

U. Klingmüller, A. Bauer, S. Bohl, P.J. Nickel, K. Breitkopf, S. Dooley, S. Zellmer, C. Kern, I. Merfort, T. Sparna, J. Donauer, G. Walz, M. Geyer, C. Kreutz, M. Hermes, F. Götschel, A. Hecht, D. Walter, L. Egger, K. Neubert, C. Borner, M. Brulport, W. Schormann, C. Sauer, F. Baumann, R. Preiss, S. MacNelly, P. Godoy, E. Wiercinska, L. Ciuclan, J. Edelmann, K. Zeilinger, M. Heinrich, U.M. Zanger, R. Gebhardt, T. Maiwald, R. Heinrich, J. Timmer, F. von Weizsäcker and J.G. Hengstler

Abstract: Complex cellular networks regulate regeneration, detoxification and differentiation of hepatocytes. By combining experimental data with mathematical modelling, systems biology holds great promises to elucidate the key regulatory mechanisms involved and predict targets for efficient intervention. For the generation of high-quality quantitative data suitable for mathematical modelling a standardised *in vitro* system is essential. Therefore the authors developed standard operating procedures for the preparation and cultivation of primary mouse hepatocytes. To reliably monitor the dynamic induction of signalling pathways, the authors established starvation conditions and evaluated the extent of starvation-associated stress by quantifying several metabolic functions of cultured primary hepatocytes, namely activities of glutathione-*S*-transferase, glutamine synthetase, CYP3A as well as secretion of lactate and urea into the culture medium. Establishment of constant metabolic activities after an initial decrease compared with freshly isolated hepatocytes showed that the cultured hepatocytes achieve a new equilibrium state that was not affected by our starving conditions. To verify the highly reproducible dynamic activation of signalling pathways in the *in vitro* system, the authors examined the JAK-STAT, SMAD, PI3 kinase, MAP kinase, NF-κB and Wnt/β-catenin signalling pathways. For the induction of gp130, JAK1 and STAT3 phosphorylation IL6 was used, whereas TGFβ was applied to activate the phosphorylation of SMAD1, SMAD2 and SMAD3. Both Akt/PKB and ERK1/2 phosphorylation were stimulated by the addition of hepatocyte growth factor. The time-dependent induction of a pool of signalling competent β-catenin was monitored in response to the inhibition of GSK3β. To analyse whether phosphorylation is actually leading to transcriptional responses, luciferase reporter gene constructs driven by multiple copies of TGFβ-responsive motives were applied, demonstrating a dose-dependent increase in luciferase activity. Moreover, the induction of apoptosis by the TNF-like cytokine Fas ligand was studied in the *in vitro* system. Thus, the mouse hepatocyte *in vitro* system provides an important basis for the generation of high-quality quantitative data under standardised cell culture conditions that is essential to elucidate critical hepatocellular functions by the systems biology approach.

IEE Proceedings online no. 20050067

doi:10.1049/ip-syb:20050067

Paper first received 18th September 2005 and in revised form 4th January 2006

U. Klingmüller, S. Bohl and P.J. Nickel are with the Boveri Group, Systems Biology of Signal Transduction, German Cancer Research Center (DKFZ), Heidelberg, Germany

A. Bauer, M. Hermes, M. Brulport, W. Schormann, C. Sauer, J. Edelmann and J.G. Hengstler are with the Center for Toxicology, Institute of Legal Medicine and Rudolf-Boehm-Institute of Pharmacology and Toxicology, University of Leipzig, Germany

K. Breitkopf, S. Dooley, P. Godoy, E. Wiercinska and L. Ciuclan are with the Department of Medicine II, Section Molecular Alcohol Research in Gastroenterology, University Hospital of Mannheim, University of Heidelberg, Mannheim, Germany

S. Zellmer and R. Gebhardt are with the Institute of Biochemistry, Medical Faculty, University of Leipzig, Leipzig, Germany

C. Kern, I. Merfort and T. Sparna are with the Department of Pharmaceutical Biology and Biotechnology, University of Freiburg, Freiburg, Germany

J. Donauer, G. Walz and M. Geyer are with the Renal Division, Department of Medicine, University Hospital Freiburg, Freiburg, Germany

C. Kreutz, T. Maiwald and J. Timmer are with the Freiburg Center for Data Analysis and Modelling (FDM), University of Freiburg, Germany

F. Götschel, A. Hecht, D. Walter, L. Egger, K. Neubert and C. Borner are with the Institute of Molecular Medicine and Cell Research, Albert-Ludwigs-University, Freiburg, Germany

F. Baumann and R. Preiss are with the Institute of Clinical Pharmacology, University of Leipzig, Leipzig, Germany

S. MacNelly and F. von Weizsäcker are with the Department of Medicine II, University of Freiburg, Freiburg, Germany

K. Zeilinger is with the Department of Experimental Surgery, University Medicine, Charite Campus Virchow, Berlin, Germany

M. Heinrich is with the Cell Techniques and Applied Stem Cell Biology, Biocity Leipzig, Leipzig, Germany

U.M. Zanger is with the Dr. Margarete Fischer-Bosch Institute of Clinical Pharmacology, Auerbachstr. 112, 70376, Stuttgart, Germany

R. Heinrich is with the Humboldt University Berlin, Math.-Nat. Department I, Institute of Biology, Theoretical Biophysics, Invalidenstrasse 42, Berlin 10115, Germany

E-mail: jan.hengstler@medizin.uni-leipzig.de

1 Introduction

Regeneration, detoxification and differentiation of hepatocytes are regulated by the highly dynamic activation and deactivation of multiple signalling pathways. The newly emerging interdisciplinary field of systems biology combines quantitative experimental data with mathematical modelling and provides the means to promote functional understanding at the systems level [1–3]. By establishing a mathematical model of the JAK2–STAT5 signalling pathway, we predicted nuclear shuttling as the most sensitive parameter to perturbations. Indeed, model prediction could be experimentally verified demonstrating that STAT5 undergoes rapid nucleocytoplasmic cycles, continuously coupling receptor activation and target gene transcription, thereby forming a remote sensor between nucleus and receptor [1]. Critical for the success of dynamic pathway modelling is high-quality quantitative data generated under standardised conditions. Hence, to elucidate complex cellular processes facilitating regeneration, detoxification and differentiation of hepatocytes by a systems biology approach it is essential to establish a standardised *in vitro* system. For the experimental validation of mathematical predictions genetically modified mice provide important tools to examine a system under perturbed conditions. Therefore the present study is focussed on establishing a highly reproducible *in vitro* system to analyse signal transduction pathways in primary mouse hepatocytes. Presently existing hepatocyte cell lines or stem cell-derived hepatocyte-like cells differ from primary hepatocytes in many relevant aspects [4–7], and thus it is important to use primary hepatocytes, that are in addition closer to the *in vivo* situation than cell lines [8–12]. It would be naive to expect that all parameters of cultured primary cells closely resemble the *in vivo* situation. Preservation of individual hepatocellular functions strongly depends on culture conditions [10, 11, 13]. For instance, hormonal additives, such as dexamethasone, as well as three-dimensional culture systems and constituents of the extracellular matrix are key elements for the maintenance of drug metabolising enzymes and further differentiated functions [14–20]. However, culture conditions including hormonal additives are not ideal for studying signal transduction, as hormones could trigger the pathways of interest. Therefore for modelling of signal transduction, culture conditions should be chosen that ensure (i) low basal activities of the pathways of interest; (ii) high, *in vivo*-like responsiveness of signal transducers to external stimuli, such as hormones and receptor ligands; (iii) reasonable maintenance of differentiated hepatocellular functions [4]; (iv) high reproducibility and (v) the possibility to harvest sufficient amounts of protein and RNA. Low basal signal transduction activities require a starving period, where hepatocytes are cultured under conditions free of serum and hormonal additives. In contrast, the absence of factors such as serum, hepatocyte growth factor (HGF), epidermal growth factor (EGF), dexamethasone, insulin, glucagon, nicotinamide, transferrin, for longer periods will compromise the hepatocytes' physiology [14, 21]. Thus, it is critical to establish starving conditions that on the one hand ensure low basal signal transduction activities, but on the other hand do not severely disturb differentiated hepatocellular functions such as metabolism, albumin secretion and urea production. Although several studies about signal transduction in mouse hepatocytes have been published [22, 23], a systematic validation of the hepatocyte culture conditions for signalling experiments has not yet been performed. Based on published media for hepatocyte culture

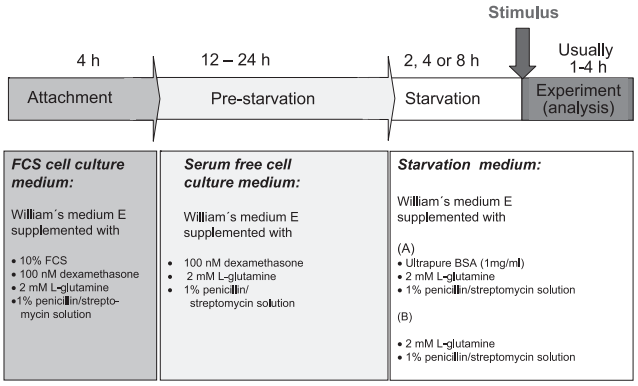

Fig. 1 *Three-step starving procedure for mouse hepatocytes*

and our own previous experiments [11, 24, 25], we established a protocol, minimising the complexity of required additives to the culture medium (Fig. 1). Here, we demonstrate that these highly reproducible and easy to handle conditions ensure responsiveness of all studied signal transduction pathways, namely the JAK–STAT, SMAD, PI3K-Akt, ras-ERK, NF-κB, Wnt/β-catenin and Fas Ligand (FasL)-induced signalling pathways.

2 Materials and methods

2.1 Materials

Ultra pure bovine serum albumin (BSA) was obtained from Sigma (A-9418, Powder cell culture tested). William's medium E (WME), dexamethasone, insulin and Percoll were obtained from Sigma (Deisenhofen, Germany), fetal calf serum (FCS) from Biochrom (Berlin, Germany) and penicillin/streptomycin (10.000 U/ml – 10 mg/ml) from Gibco (Paisley, Scotland). Materials used for hepatocyte isolation and culture were 26G × 1/2 needles (Sterican, Braun, Melsungen, Germany), Scalpels (no. 11; Feather PFM, Cologne, Germany), Abbocath-T 18G (Venisystems, Abbott, Ireland), Peristaltic pumps (Reglo Digital; Isamtech, Zürich, Switzerland), 100 μm meshcell strainers (Becton-Dickinson), collagen I coated six-well-plates (Becton-Dickinson) and tissue culture centrifuges (Labofuge M, Heraeus, Stuttgart, Germany). All other chemicals of analytical grade were obtained from Merck (Darmstadt, Germany).

2.2 Hepatocyte isolation and culture

Isolation and culture of mouse hepatocytes was performed according to standard operation procedures (SOP hepatocyte isolation and SOP hepatocyte culture in Supplementary Materials section). Six- to 12-week-old B6 mice were used. The use of mice for hepatocyte isolation has been approved by the animal experimental committees and animals were handled and housed according to specific pathogen-free conditions. Anaesthesia was achieved by intraperitoneal injection of 5/100 mg body weight ketamine hydrochloride 10% (115.34 mg/ml; Essex Tierarznei, Munich, Germany) and 1/100 mg body weight xylazine hydrochloride 2% (23.32 mg/ml; Bayer Leverkusen). HANKS solution I was produced by supplementation of BASAL HANKS solution (8 g NaCl, 0.4 g KCl, 3.57 g Hepes, 0.06 g $Na_2HPO_4 \times 2H_2O$, 0.06 g KH_2PO_4 in 1 l distilled H_2O, adjusted pH to 7.4, sterilised) with 2.5 mM EGTA, 0.1% glucose and penicillin/streptomycin at a dilution of 1:100. HANKS solution II was produced by

supplementation of BASAL HANKS solution with 0.3 mg/ml collagenase CLSII and 5 mM $CaCl_2$. Hanks solutions I and II were prewarmed in a 42°C waterbath. Collagenase was added immediately prior to liver perfusion. After shaving and cleaning the abdomen under sterile conditions, the abdominal cavity was opened and the portal vein was cannulated with a 24G catheter. A silicon tube (diameter 2.4 mm) was connected to the catheter and HANKS solution I was infused using a peristaltic pump at a flow rate of 8 ml/min. After starting the peristaltic pump, the vena cava and the right heart ventricle were incised to permit sufficient outflow. The liver was perfused with solution I for 2 min, followed by HANKS solution II for 5–7 min. Correct placement of the portal vein catheter is evidenced during perfusion by the steady and even change from dark red-brown to a light brown color in all liver lobes. Following perfusion, the liver was transferred to a sterile Petri dish and the gall bladder was removed. The following steps were performed in a sterile hood. The liver capsule was carefully removed using a pincette. Gentle shaking disintegrated the perfused liver, yielding a suspension of single cells, some cell clumps and cell debris. The suspension was placed onto a 100 μm cell strainer and was filtered through the mesh by gravity flow. The suspension was transferred to a 50 ml Falcon tube and washed twice with WME (room temperature). Cells were centrifuged at room temperature at 37.5*g* for 2 min in a cell culture centrifuge. The cells were resuspended in WME and the percentage of intact cells was determined by staining an aliquot with trypan blue. On an average 70–80% of the cells were viable. Hepatocytes were plated on collagen-coated tissue culture dishes in FCS cell culture medium (WME supplemented with 10% FCS, 100 nM dexamethasone, 2 mM L-glutamine and 1% penicillin/streptomycin solution) and kept in a humidified cell culture incubator at 37°C and 5% CO_2 (Fig. 1). For 9 cm (diameter) tissue culture dishes, hepatocytes were plated at a density of 5×10^6 cells/dish in 10 ml FCS culture medium. For six-well plates, 1×10^6 cells/dish were plated in 3 ml FCS culture medium. After 4 h of incubation, hepatocytes should be attached to the collagen-coated dish. Subsequently, the FCS cell culture medium was removed and replaced by serum-free cell culture medium (WME supplemented with 100 nM dexamethasone, 2 mM L-glutamine and 1% penicillin/streptomycin solution). After 14–20 h in serum-free cell culture medium (usually overnight) hepatocytes were washed three times with starvation medium (WME supplemented with 2 mM L-glutamine and 1% penicillin/streptomycin solution, with or without 1 mg/ml ultrapure BSA as indicated in Section 3). Subsequently, hepatocytes were incubated in starvation medium for the time periods given in Section 3. For stimulation, either 40 ng/ml IL-6 for 10 min, 1 ng/ml TGF-β for 60 min, 10 ng/ml EGF for 20 min and 200 nM insulin for 20 min were added to the starvation medium. For induction of cell death, hepatocytes were treated with conditioned medium from mouse FasL-producing/secreting Neuro-2a cells [26].

2.3 Percoll purification

For some initial experiments, the hepatocyte suspensions were further purified by centrifugation in Percoll adjusted to a density of 1.065 g/ml for 10 min at 50*g*. With this method the total yield of cells was reduced by up to 50% but the contamination with non-parenchymal cells is lower than 1%.

2.4 Cell lysis

The medium was completely removed and cells were lysed with 500 μl 1% NP-40 lysis buffer (1% NP-40, 150 mM NaCl, 20 mM Tris–HCl pH 7.4, 10 mM NaF, 1 mM EDTA pH 8.0, 1 mM $ZnCl_2$ pH 4.0, 1 mM $MgCl_2$, 1 mM Na_3VO_4, 10% glycerol) supplemented with protease inhibitors (aprotinin, AEBSF). Cells were detached and lysates were transferred to microcentrifuge tubes. After rotation for 20 min at 4°C, lysates were centrifuged at 20 000*g*, 10 min, 4°C (Eppendorf 5417R) to remove cell debris. The cleared supernatants were transferred to fresh tubes and protein concentrations were determined by Bradford analysis.

For the analysis of β-catenin signalling, hepatocytes were kept in serum-free media for 4 h after plating, before being starved for 16 h. To activate β-catenin signalling, cells were treated with 80 μM SB216763 (stock solution 10 mM in DMSO; Sigma–Aldrich) for different lengths of time. Control cells received an equivalent volume of DMSO. Protein extracts were prepared by lysing cells in ice-cold IPN150 buffer (50 mM Tris–HCl pH 7.6, 5 mM $MgCl_2$, 0.1% NP-40, 150 mM NaCl, 1 mM DTT, 0.1 mM Na-Vanadate, 10 mM NaF, 1 mM PMSF) and complete protease inhibitor (Roche Applied Science) for 30 min on ice with occasional mixing. After cell lysis, samples were centrifuged at 20 000*g* for 10 min and the protein concentration of the cleared supernatant was determined (DC protein assay, BioRad).

2.5 Immunoprecipitation and immunoblotting

For the detection of phosphorylated and total STAT3 and SMAD2/3, cleared cell lysates were rotated with 25 μl protein A sepharose (GE Healthcare Systems) and antibody (STAT3 Cell Signaling Technologies; SMAD Santa Cruz Biotechnologies) overnight at 4°C. Immunoprecipitates were washed twice with 1% NP-40 lysis buffer and once with TNE (10 mM Tris–HCl pH 7.4, 100 mM NaCl, 1 mM EDTA, 100 μM Na_3VO_4). The pellets were resuspended in 25 μl 2× sample buffer (4% SDS, 100 mM Tris–HCl pH 7.4, 20% glycerin, 200 mM DTT, 0.02% bromophenol-blue, 10% β-mercaptoethanol) and boiled at 95°C for 2 min. After centrifugation at 16 000*g* for 2 min, the supernatant was separated on 10% SDS–PAGE and transferred to nitrocellulose membranes (Schleicher-Schuell) by semi-dry transfer (Hoefer TE 77). Signals were detected using the ECL advance detection kit (GE Healthcare Services) in combination with LumiImager (Roche Diagnostics) and quantified by the LumiAnalyst software (Roche Diagnostics). For time-course analysis, the quantitative data was processed as described previously [27]. For the analysis of SMAD1 in comparison to SMAD2, hepatocytes were serum-starved (0.5% FCS) for 16 h, followed by stimulation with 5 ng/ml TGF-α (PeproTech EC, London, UK) for 1, 2 and 6 h and lysed in RIPA lysis buffer containing protease and phosphatase inhibitor cocktails (Sigma, Steinheim, Germany). Total protein lysates of 20 μg were separated on a 4–12% Bis–Tris gradient-gel (Invitrogen, Carlsbad, CA, USA) and blotted onto nitrocellulose membrane (Protran, Schleicher&Schrell BioScience, Dassel, Germany) by a tank-blot transfer system (Invitrogen, Carlsbad, CA, USA). By enhanced chemiluminescence (Super Signal West Dura Extended Duration Substrate, Pierce, Rockford, IL, USA), proteins were detected using the following antibodies: pSMAD1 and pSMAD2 (Cell Signaling Technology, Beverly, MA, USA), SMAD2,

(Zymed, South San Francisco, CA, USA); β-actin (Sigma, Steinheim, Germany).

The analysis of phosphorylated and total Akt and ERK1/2 was performed as previously described [28, 29]. Briefly, total cellular lysate (50 μg) was mixed with sample buffer [30], resolved on a 12% SDS-polyacrylamide gel by electrophoresis and transferred onto Poly Screen polyvinylidene-difluoride (PVDF) transfer membranes (NEN® Life Science, Boston, MA, USA). Membranes were blocked with PBST (PBS + 0.1% Tween-20) containing 10% Roti®-Block (Roth, Karlsruhe, Germany) for 1 h and then incubated with the corresponding primary antibodies [ERK2: Santa Cruz Biotechnology Inc., Santa Cruz, CA, USA; phospho-p44/p42 MAP Kinase (p-ERK1/2), phospho-Akt and Akt: Cell Signalling Technology, New England Biolabs GmbH, Frankfurt, Germany; β-actin: Sigma]. Incubation time was 2 h at room temperature for ERK2 antibodies, 30 min at room temperature for β-actin antibodies (loading control) and overnight at 4°C for t phospho-Akt and Akt antibodies. After washing, membranes were incubated with secondary antibody, horseradish peroxidase- conjugated anti-mouse immunoglobulin or anti-rabbit immunoglobulin at room temperature (rabbit anti-mouse IgG: Sigma; sheep anti-rabbit IgG: Chemicon International Inc., Hofheim/Ts, Germany and goat anti-rabbit IgG: Cell Signalling Technology). After final washing, proteins were visualised with a chemiluminescence detection system (Western Lightning™ Chemiluminescense Reagent Plus, Perkin-Elmer Life Science, Boston, MA, USA) in combination with INTAS Chemi Lux Imager System (INTAS Science Imaging Company, Göttingen, Germany) and quantified by the Gel-Pro Analyzer software Analyst software (INTAS Science Imaging Company, Göttingen, Germany). The MagicMark™ Western Standard (Invitrogen GmbH, Karlsruhe, Germany) served as an internal protein standard [30]. For repeated staining, individual membranes were stripped with a Restore™ Western Blot Stripping Buffer (Perbio Science Deutschland GmbH, Bonn, Germany) for 30 min at 37°C [31, 32].

To analyse total cellular β-catenin levels, 20 μg protein of cellular lysates were separated by SDS–PAGE on 10% gels. Prior to loading, each sample received a mixture with 2.5 and 1.25 ng of GST fusion proteins carrying amino acid residues 1–150/577–781 and 536–781 of β-catenin, respectively. These calibrator proteins served to monitor the efficacy of the immunoblotting procedure and allowed normalisation of the results upon quantification. After transfer to PVDF membranes, immunoblots were sequentially probed with anti-β-catenin primary antibodies (clone 14, BD Pharmingen), anti-actin primary antibodies (MP Biomedicals Inc.), and the appropriate horseradish peroxidase-labelled secondary antibodies (Jackson ImmunoResearch Laboratories). Antibody/antigen complexes were visualised by chemiluminescence (ECL plus system, Amersham Pharmacia). For affinity precipitation of the free cytoplasmic pool of β-catenin, 3 μg of the GST–ECT fusion protein, 12.5 μl bed volume of glutathione sepharose beads and cellular lysate with a protein content of 1000 μg were combined. In addition, all samples received 5 ng of the GST–β-catenin calibrator protein with amino acid residues 1–150/577–781 to monitor the efficacy of GST fusion protein recovery. The assay volume was adjusted to 750 μl with IPN150. Binding reactions were incubated at 4°C with constant agitation overnight. Following extensive washing with IPN150, material retained on the glutathione sepharose was eluted in SDS–PAGE loading buffer, and equal amounts of the GST–β-catenin calibrator protein with amino acid residues 536–781 were added to all samples. Protein mixtures were then separated by SDS–PAGE on 10% gels and analysed by immunoblotting as earlier. Chemiluminescent images were quantified using the LumiImager and the LumiAnalyst Software (Roche Applied Science).

2.6 Expression and purification of glutathione-S-transferase (GST) fusion proteins

Expression vectors for GST fusion proteins with β-catenin residues 536–781, and the cytoplasmic tail of E-cadherin (GST–ECT) have been described [33, 34]. A construct for expressing GST–β-catenin amino acid residues 1–150 fused to 577–781 was obtained by deleting a PmlI/Ecl136II restriction fragment from pGEX4T1-β-catenin [33]. GST fusion proteins were expressed in *Escherichia coli* BL21 and purified on glutathione sepharose as described [33].

2.7 TGF-β reporter assays

Freshly isolated hepatocytes were plated on black collagen-coated 96-well-plates at a density of 1.5×10^4 cells per well in FCS cell culture medium. After 4 h, FCS cell culture medium was replaced by serum free cell culture medium, cells were infected with 1.5×10^6 infectious viral particles/well and were stimulated with TGF-β 12 h later. Adenoviruses expressing luciferase driven by either multiple copies of a TGF-β response and SMAD3/4 binding element ('CAGA-Luc'), which had originally been isolated from the human PAI-1 promoter or driven by a palindromic repetition of a SMAD1/5 binding cassette from the mouse Id1-promoter ('BRE-Luc'; [35]) were used. Viruses were purified using the BD Adeno-X Virus Purification kit (Q-Biogene, Heidelberg, Germany). After infection, hepatocytes were stimulated with the indicated amounts (0.5–10 ng/ml) of recombinant human TGF-β_1 (R&D) for 3–4 h. Cell lysis occurred directly in the wells and total luciferase activity per well was measured (using the Steady-Glo Luciferase Assay System; Promega, Madison, WI, USA). To compare the results of different experiments, all values were normalised to the corresponding (untreated) control. Infection rates in each experiment were constantly higher than 90% of the cells, as determined by a corresponding GFP-adenovirus. In addition to the CAGA construct, a SMAD1/5 responsive luciferase construct was used as described by Korchynskyi *et al.* [35]. Adenoviral infection of hepatocytes was performed at two different time points: (i) immediately after the attachment of the hepatocytes (4 h after plating) in serum-free cell culture medium. Thus, stimulation with TGF-β_1 and analysis of luciferase activity was performed at day 1 of hepatocyte culture (whereby day 0 is defined as the day of hepatocyte isolation); and (ii) at day 2 of hepatocyte culture. For day 2 hepatocytes were cultured for additional 24 h in FCS cell culture medium after the 4 h attachment period, followed by adenoviral infection in serum-free cell culture medium.

2.8 RT–PCR

Total RNA was isolated using the High Pure RNA isolation kit (Roche, Mannheim) from hepatocytes after different times of primary culture as indicated. Total RNA of 1 μg was reverse-transcribed into cDNA (total volume 20 μl

for 1-day-old cultures and 40 μl for percoll-purified cells) and 1 μl was analysed by PCR (30 cycles). Primer sequences were as follows:

Primers (mouse)	Sequence (5′ = >3′)
β-Actin	
Forward	CACCCACACTGTGCCCATC
Reverse	CTCCTGCTTGCTGATCCAC
Albumin	
Forward	GCACACAAGAGTGAGATCGC
Reverse	TCTGCATACTGGAGCACTTC
Cytokeratin-18	
Forward	CAAGATCATCGAAGACCTGAG
Reverse	CCTCAATCTGCTGAGACCAG
Desmin	
Forward	CTACTCGTCCAGCCAGCG
Reverse	CGGATCTCCTCTTCATGCAC
Fibrinogen Bβ	
Forward	GAGACATCCGAAATGTATCTC
Reverse	GAGTACCACGATCCCTTCC
Transferrin	
Forward	GTATTATGCCGTGGCTGTGG
Reverse	GCTTGGGCCAGGTGGCAG
α-SMA	
Forward	GTGCTGGACTCTGGAGATG
Reverse	CCACCGATCCAGACAGAGTA
TGF-β1	
Forward	GGTCACCCGCGTGCTAATG
Reverse	CAGAAGTTGGCATGGTAGCC

2.9 Electrophoretic mobility shift assays

Hepatocytes were cultured in six-well-plates at a density of 1 million cells per well. After 2–3 h in FCS free cell culture medium, they were washed with PBS and incubated in starvation medium (WME supplemented with 2 mM L-glutamine and 1% penicillin/streptomycin solution without 1 mg/ml ultrapure BSA) for 24 h. For stimulation experiments, 1 ng/ml TNF-α was added to the culture medium for different periods as indicated. Total cell extracts were prepared with a high-salt detergent buffer (Totex: 20 mM Hepes, pH 7.9, 350 mM NaCl, 20% (v/v) glycerol, 1% (w/v) Nonidet P-40, 1 mM $MgCl_2$, 0.5 mM EDTA, 0.1 mM ethylene glycol-bis-(β-aminoethyl ether) *N*,*N*,*N*′,*N*′ tetraacetic acid, 0.5 mM DTT, 0.1% phenylmethylsulfonyl fluoride, 1% aprotinin). Briefly, starvation medium was removed and cells were washed with 1 ml ice-cold PBS. Then, lysis was started by the addition of 100 μl of Totex buffer to each plate and finished after 30 min incubation on ice by scraping. Cell lysates were collected in eppendorf tubes and centrifuged for 5 min at 16 000*g* and 4°C. Nuclear extracts were prepared as follows. Cells were washed in the well once with ice-cold PBS and incubated with buffer A (10 mM Hepes pH 7.6, 15 mM KCl, 2 mM MgCl, 0.1 mM EDTA pH 8.0) on ice for 10 min. Then buffer A was replaced by 300 μl Igepal (buffer A, 0.2% NP-40), incubated for 5 min on ice, and transferred into Eppendorf tubes. After centrifugation (2000 *g*, 4°C, 5 min), pellets were stored for further extraction. The same wells were washed again with buffer C and then incubated with 50 μl buffer C (25 mM Hepes pH 7.6, 50 mM KCl, 0.1 mM EDTA pH 8.0, 10% glycerol, protease inhibitors). After 5 min on ice, 4.5 μl 5 M NaCl were added and the nuclei were incubated for further 5 min. Subsequently, nuclei, which were still left in the wells, were scraped off, unified with the pellet, vortexed and incubated with gentle shaking at 4°C for 20 min. After centrifugation (5800 *g*, 4°C, 10 min), the supernatant was stored at −80°C for further studies. For electrophoretic mobility shift assays (EMSAs), 5 μl of the stored supernatant (nuclear extract; 5–15 μg protein) were added to a reaction mixture containing 20 μg BSA (Sigma), 2 μg poly(d*I*–d*C*) (Roche Molecular Biochemicals), 2 μl buffer D+ (20 mM Hepes, pH 7.9, 20% glycerol, 100 mM KCl, 0.5 mM EDTA, 0.25% Nonidet P-40, 2 mM DTT, 0.1% phenylmethylsulfonyl fluoride), 4 μl buffer F (20% Ficoll 400, 100 mM Hepes, 300 mM KCl, 10 mM DTT, 0.1% phenylmethylsulfonyl fluoride) and 100 000 cpm (Cerenkov) [^{33}P]-labelled oligonucleotide, made up to a final volume of 20 μl with distilled water. NF-κB oligonucleotide (Promega) was labelled using [γ-33P] dATP (3000 Ci/mmol; Amersham) and a T4 polynucleotide kinase (New England Biolabs). Sample and reaction mixture were incubated for 25 min at room temperature and loaded on a non-denaturating 4% polyacrylamide gel. Separation was run at 200 V (22–14 mA) for 90 min. The gel was transferred to a Whatman 3 mm paper and dryed under vacuum at 80°C for 75 min. After drying, the gel was exposed to a Phosphoimager BAS film (Fujifilm) for 24 h. Detection was performed by a Phosphoimager (Fujifilm).

2.10 His-annexin-V-GFP and propidium iodide (PI) staining

Cells were seeded on 12 mm glass coverslips according to the SOPs and cultivated for 36 h. After starvation for 12 h, the cells were incubated with FasL for 1, 3 and 6 h or left untreated. The hepatocytes were stained with 3 μg/ml His-annexin-V-GFP [36] and 2.5 μg/ml PI (Sigma) in annexin V binding buffer (10 mM Hepes/NaOH, pH 7.4, 140 mM NaCl, 2.5 mM $CaCl_2$) prior to fixation with 4% paraformaldehyde (PFA) containing 2 μg/ml DNA-stain Hoechst 33342 (Sigma–Aldrich). Coverslips were viewed under a confocal ZEISS LSM 510 META microscope (Zeiss) with a plan-neofluar 40×/NA 1.3 oil immersion objective. GFP molecules were excited with the 488 line of a krypton–argon laser and imaged with a 505–530 bandpass filter. PI was excited with the 488 line and imaged with a 560 longpass filter. Hoechst dye was excited with a fluorescent lamp and imaged with a 475 longpass filter. Image capturing, processing and automatic and manual data acquisition were performed using the Zeiss LSM Image Browser 3.5.

2.11 DNA fragmentation

According to the SOPs, 2×10^6 cells were plated on collagen I- coated 6 cm dishes (Bioware), cultivated for 36 h and starved for 12 h. Subsequently, the cells were incubated with FasL [26] for 1, 3 and 6 h or left untreated. After washing in PBS, the cells were resuspended in RIPA buffer (50 mM Tris pH 7.5, 150 mM NaCl, 1% NP40, 0.5% sodium deoxycholate, 0.1% SDS) and incubated for 20 min at 4°C. After centrifugation for 10 min at 20 000*g* at 4°C (Eppendorf centrifuge 5417 R), the supernatant was used for chloroform–phenol extraction (phenol–chloroform–isoamylalcohol 23 : 24 : 1, Roth). After centrifugation for 5 min at 2700*g*, the aqueous phase was adjusted to 0.3 M NaAc and DNA was precipitated adding two volumes of 100% ethanol (−20°C), washed in

70% ethanol and air-dried. The pellet was resuspended in TE-RNAseA (25 μg/ml) and incubated for 30 min at 37°C. Five micrograms of DNA were separated on a 1.7% agarose gel in 1% TAE buffer. The picture was taken using the LumiImager (Roche).

2.12 Enzyme activities

Glutamine synthetase activity was determined according to the γ-glutamyltransferase assay of Levintow [37] with modifications decribed by Gebhardt and Williams [38]. Briefly, 100 μl hepatocyte homogenate were incubated with 400 μl working solution composed of 50 mM imidazole, 50 mM L-glutamine, 25 mM hydroxylamine hydrochloride, 0.16 mM ADP, 25 mM sodium arsenate and 1 mM $MnCl_2$ (final concentration, pH 6.8) at 37°C for 15–30 min. The reaction was stopped by the addition of 1 ml stop-mix, composed of 1.83 N HCl, 1.45% TCA and 2.4% $FeCl_2$. Blanks were prepared by the addition of stop-mix before the addition of working solution. The samples were centrifuged to remove cell debris and the extinction was determined at 540 nm. Activities of CYP3A (6-β-hydroxylation of testosterone) GST [substrate: 1-chloro-2-4-dinitrobenze (CDNB)] were determined as previously described [15, 16].

3 Results

3.1 Normal hepatocyte morphology and basal hepatocellular functions despite starvation conditions

Despite a 12–24 h period in pre-starvation medium and up to 8 h in starvation medium (Fig. 1), mouse hepatocytes showed a normal morphology with polygonal cells and frequently two or more nuclei per cell (Fig. 2*a*). No major differences in activities of CYP3A (6-β-hydroxytestosterone), GST, glutamine synthetase and urea secretion were observed between hepatocytes continuously cultured in FCS cell culture medium for 40 h when compared with hepatocytes kept in pre-starvation (16 h) and BSA-free starvation medium (24 h) (Table 1). RT–PCR demonstrated expression of typical hepatocyte markers like albumin, cytokeratin 18, fibrinogen and transferrin (Fig. 2*b*). α-SMA and desmin are typically expressed by non-parenchymal liver cells and not by hepatocytes but it is well-known that hepatocytes isolated by collagenase perfusion contain approximately 2% of non-parenchymal cells [14]. Therefore the weakly positive RT–PCR data for α-SMA and desmin at day 1 are not surprising and are detectable only due to the high sensitivity of this method. Percoll purification of isolated liver cells represents a technique that allows enrichment of viable hepatocytes and further decreases the fraction of non-parenchymal cells [11, 12]. Accordingly, negative α-SMA and desmin RT–PCR data were obtained for Percoll purified hepatocytes at least up to 48 h in culture (Fig. 2*c*). However, after a culture period of 72 or 96 h, respectively, α-SMA and desmin were detectable again, suggesting that a small fraction of non-parenchymal cells remained in spite of Percoll centrifugation and proliferated during the culture period. Absence of TGF-β1 expression in hepatocytes is in accordance with published data [39]. In the present study, we focus on key factors of signal transduction that were analysed by immunoblotting. For this type of analysis the small fraction of non-parenchymal cells did not influence the results (data not shown). Therefore all further experiments were performed using hepatocyte preparations without Percoll purification.

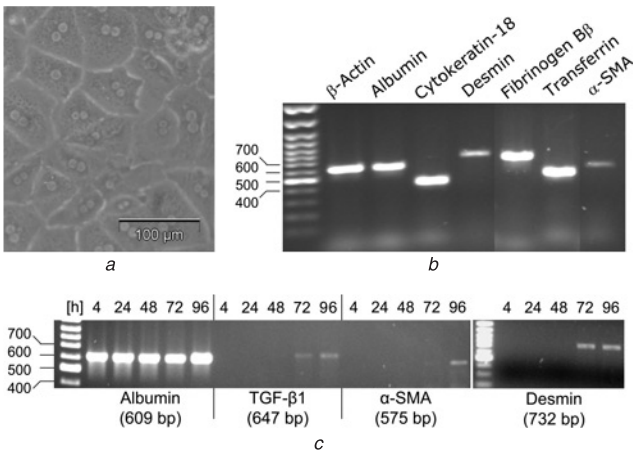

Fig. 2 *mRNA expression and morphology of mouse hepatocytes cultured on collagen-coated Petri-dishes after starvation*

a Morphology of mouse hepatocytes after attachment (4 h), pre-starvation (16 h) and 8 h of starvation

b RT–PCR analysis demonstrating expression of hepatocyte markers Total RNA of 1 μg isolated from hepatocytes after 1 day in culture, was reverse-transcribed into cDNA. Expression of hepatocyte marker genes was determined by PCR as described in Section 2

c Expression of α-smooth muscle actin (α-SMA), desmin, albumin and TGF-β1 in mouse hepatocytes cultured after additional purification by Percoll centrifugation

Expression of the non-parenchymal cell markers α-SMA, desmin and TGF-β1 was initially negative but became detectable after 3 to 4 days in culture implying a small remaining fraction of non-parenchymal cells

3.2 Influence of culture and starving conditions on metabolic functions of hepatocytes

Metabolic functions of cultured primary hepatocytes were quantified: (i) immediately after isolation of hepatocytes; (ii) 4 h after plating of the cells in FCS cell culture medium; (iii) after further 20 h in serum-free cell culture medium. Afterwards, hepatocyte cultures were incubated for 2, 4, 8 and 48 h in three different media: (a) starvation medium with the addition of 1 mg/ml ultrapure BSA to test whether addition of BSA supports hepatocyte integrity; (b) starvation medium without BSA; and (c) FCS cell

Table 1: Activities of GST, CYP3A and glutamine synthetase as well as urea secretion of hepatocytes cultured for 16 h in pre-starvation and 24 h in BSA-free starvation medium when compared with hepatocytes continuously kept in FCS cell culture medium for 40 h (mean values and standard deviations of three independent experiments)

	FCS cell culture medium (40 h)	Pre-starvation (16 h) plus starvation (24 h)
GST (μmol/min/mg protein)	0.66 ± 0.12	0.72 ± 0.07
CYP3A (6-β hydroxytestosterone) (nmol/min/mg protein)	0.18 ± 0.07	0.12 ± 0.02
Glutamine synthetase (mU/mg protein)	4.66 ± 1.88	7.04 ± 0.25
Urea secretion (mg/dl/24 h)	9.00 ± 0.72	9.37 ± 1.26

culture medium. The rationale of this experiment was to identify a possible influence of BSA, because several scientists add BSA to their starving media. In addition, we were interested in a possible influence due to FCS and 100 nM dexamethasone, as both were present during the attachment of hepatocytes. Similar influences of the different culture conditions were observed for activities of GST and glutamine synthetase (Figs. 3*a* and *b*). Compared with freshly isolated hepatocytes, activities decreased during the first 24 h of culture, reaching a new plateau at later stages. No major differences in activities were observed between hepatocytes cultured in starvation medium with or without BSA (Figs. 3*a* and *b*). Similarly, no obvious differences in activities occurred if hepatocytes were cultured in starvation medium or in full FCS cell culture medium containing 10% FCS and 100 nM dexamethasone. To analyse whether new levels of metabolic activities reached after 1–2 days in culture are stable, we performed incubations for up to 6 days using cell culture medium with and without addition of 10% FCS (Figs. 4*a*–*d*). Activities of CYP3A, GST and glutamine synthetase decreased during day 1–2, but reached a plateau which remained constant up to 6 days (Fig. 4).

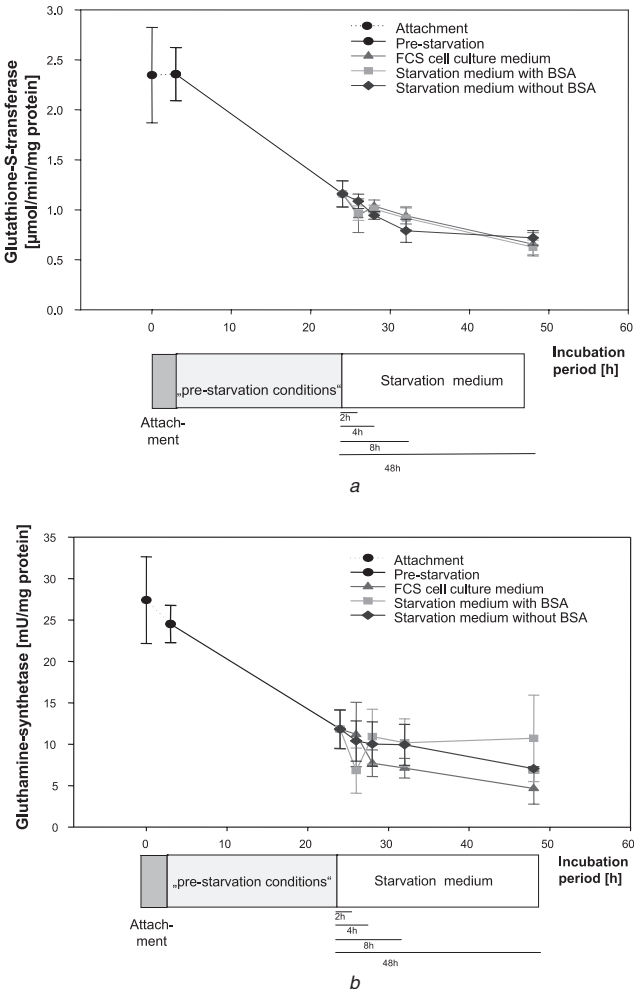

Fig. 3 *Influence of starving conditions on activities of GST (a) and glutamine synthetase (b)*

All activities were quantified (i) immediately after isolation of hepatocytes, (ii) 4 h after plating of the cells in FCS cell culture medium, (iii) after further 20 h in serum-free cell culture medium
Afterwards, hepatocyte cultures were incubated for 2, 4, 8 and 48 h in three different media: (a) starvation medium with addition of 1 mg/ml ultrapure BSA, (b) starvation medium without BSA and (iii) FCS cell culture medium to be able to identify the influence of 10% FCS and 100 nM dexamethasone

3.3 IL-6 and TGF-β activate JAK–STAT and SMAD signalling cascades

To examine signalling pathways activated during the priming or terminating phase of hepatocyte regeneration, we determined interleukin (IL)-6-induced activation of the

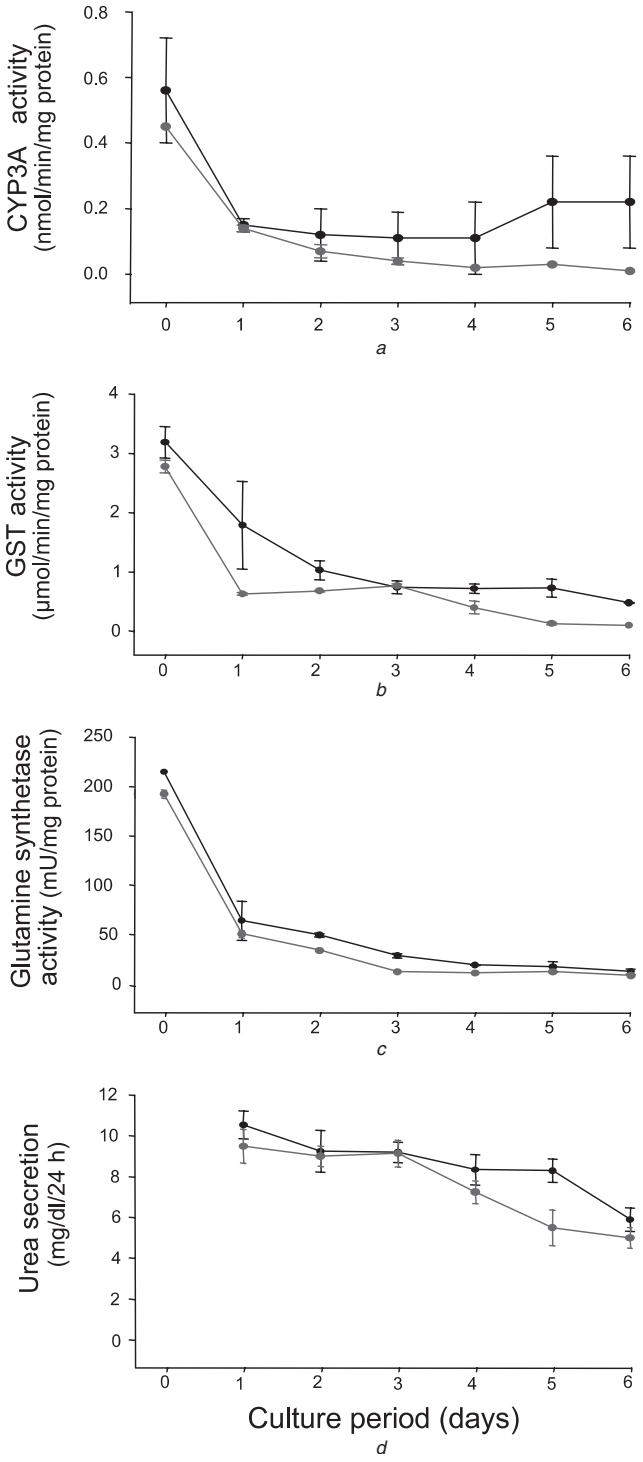

Fig. 4 *Metabolic activities for up to 6 days using cell culture medium with and without the addition of 10% FCS*

a CYP3A (6-β-hydroxylation of testosterone)
b GST
c glutamine synthetase
d urea secretion
Urea was quantified after periods of 24 h, when the culture medium was replaced. Therefore quantification at time point zero was not possible, in contrast to the enzyme activities (*a*–*c*) that could be measured also in freshly isolated hepatocytes. Black symbols: cell culture medium with 10% FCS; red symbols: cell culture medium without FCS

JAK1–STAT3 signalling pathway and the TGF-β-induced SMAD signalling cascade, respectively. As an indicator for the activation of signal transduction in our *in vitro* system the ligand-induced phosphorylation of signalling components from both cascades were examined. To test for the reproducibility of our protocol, cells from three animals were kept in starvation medium for 5 h and subsequently stimulated with IL-6 (40 ng/ml) for 10 min or TGF-β1 (8 ng/ml) for 60 min. Cellular lysates were subjected to immunoprecipitation using antibodies recognising components of IL-6 receptor–JAK1–STAT3 or SMAD signalling pathways followed by immunoblotting (Fig. 5*a*). As demonstrated by the analysis of untreated samples, our starvation protocol enabled us to reduce endogenous phosphorylation to undetectable levels for both signalling pathways. Quantitative analysis with the LumiImager revealed that phospho-specific signals were induced by ligand stimulation ranging from 2.7-fold for JAK1 to 11-fold for p-STAT3 compared with background levels (Fig. 5*b*), whereas total protein levels remained constant. Similarly, for SMAD proteins the phospho-specific signals increased by 11.8-fold for SMAD2 and 12.7-fold for SMAD3. Thus, our *in vitro* system permits the efficient induction of the JAK1–STAT3 and the SMAD signalling cascades and thereby the quantitative analysis of both pathways in primary hepatocytes.

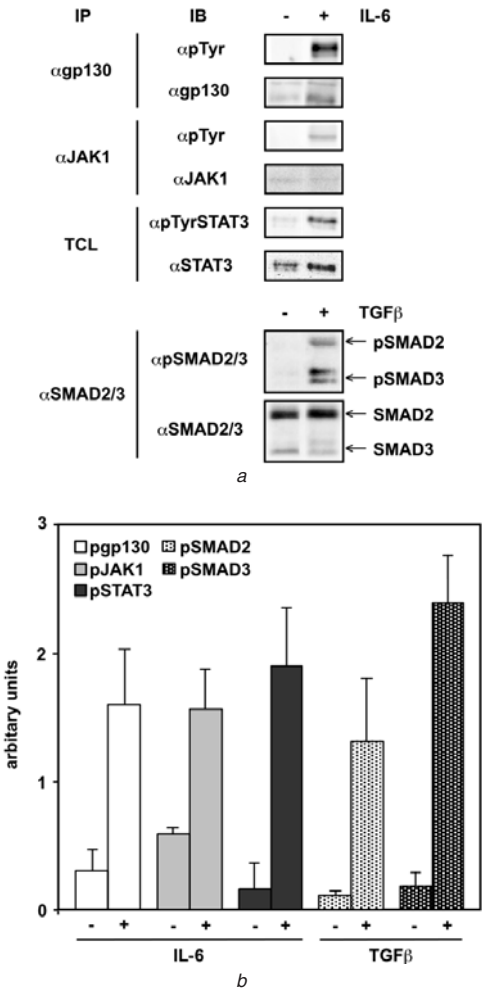

Fig. 5 *Activation of JAK–STAT and SMAD signalling pathways in primary hepatocytes*

Primary hepatocytes were isolated from three 7-week-old male BL-6 mice by two-step collagenase perfusion, cultured in FCS cell culture medium and serum-free cell culture medium according to the schedule in Fig. 1, followed by a 5 h starving period

Subsequently, 2×10^6 cells were either stimulated with 40 ng/ml IL-6 for 10 min (+), 1 ng/ml TGF-β1 for 1 h (+) or left untreated (−)

After lysis with 1% NP-40 lysis buffer, proteins were immunoprecipitated with αgp130, αJAK1 and αSMAD2/3 antibodies and separated on 10% SDS-PAGE

a After transfer to nitrocellulose membranes, phosphorylation levels were analysed by αphospho-tyrosine, αphospho (Y705) STAT3 and αphospho (S433/435)SMAD2/3 antibodies

Blots were stripped and reprobed with respective αgp130, αJAK1, αSTAT3 and αSMAD2/3 antibodies

b Quantification was performed using ECL advance detection kit in combination with LumiImager detection (arbitrary units)

The signals are represented as the average of three different preparations, error bars are shown as SD

3.4 *TGF-β1 rapidly induces phosphorylation of SMAD1 and 2*

Further, we tested whether in hepatocytes TGF-β in addition to SMAD2 also activates SMAD1. We directly compared phosphorylation of SMAD1 and 2 in total cell lysates by immunoblot analysis using specific antibodies (Fig. 6). Both SMADs were found to be phosphorylated after stimulation with TGF-β1. Although SMAD1 phosphorylation remained stable up to 6 h after stimulation, SMAD2 phosphorylation decreased to almost basal levels between 2 and 6 h. Our results indicate that phosphorylation of SMAD1 and/or SMAD2 can be quantified using our *in vitro* system.

3.5 *TGF-β-induced SMAD signalling leads to activation of artificial response elements*

Next, we analysed whether TGF-β-induced phosphorylation of R-SMADs actually leads to transcriptional responses in primary hepatocytes. The activation of transcription was measured using recombinant adenoviruses encoding a reporter gene (luciferase) which is driven by multiple copies of a TGF-β responsive motif ('CAGA', see Section 2 for details). Luciferase activities of untreated cultures or after 3 h treatment with increasing amounts of TGF-β_1 were measured in cellular lysates (Fig. 7). The

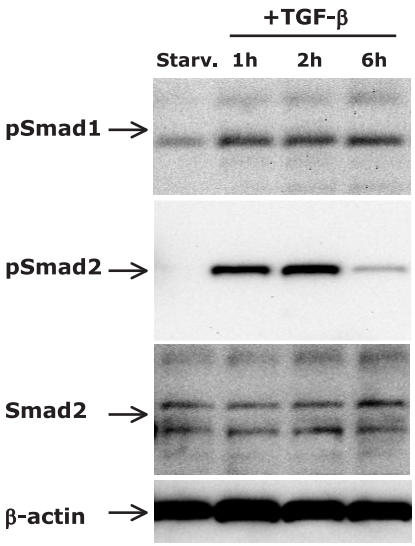

Fig. 6 *SMAD phosphorylation after TGF-β1 stimulation*

Hepatocytes were cultured in FCS cell culture medium und serum-free cell culture medium according to the schedule in Fig. 1, followed by a 12 h starving period and stimulation with TGF-β1 (5 ng/ml) for the indicated time periods

Total protein was isolated, separated on 4–12% PAA gradient gels under reducing conditions

Detection of pSMAD1 and −2, total SMAD2 and β-actin as a loading control was performed by immunoblot analysis

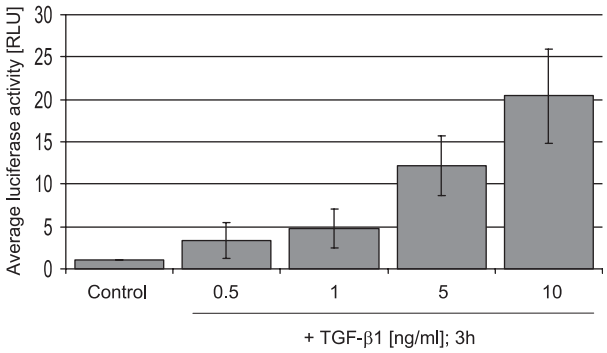

Fig. 7 *TGF-β reporter gene assay*

Hepatocytes were infected with adenoviruses encoding luciferase as a reporter gene
Luciferase expression is controlled by multiple copies of a TGF-β response motif ('CAGA-Luc') that binds SMAD3/4 complexes
One day later (at day 2 in culture), the cells were stimulated with TGF-β1 (0.5–10 ng/ml) for 3 h followed by cell lysis and measurement of luciferase activity
The graph shows the average values $\pm$SD (normalised to the untreated control) of three independent cell isolations
Each individual measurement was performed in triplicates
RLU, relative light units

dose-dependent increase in luciferase activity demonstrates a TGF-β_1 dependent formation of transcriptionally active SMAD3/4 complexes in hepatocytes. To study the influence of the culture period on signal transduction, we performed reporter assays at day 1 and day 2 of hepatocyte culture, using 'CAGA' as well as BRE-luciferase constructs (the latter one representing an artificial SMAD1/5 response cassette). A concentration-dependent increase in luciferase activity of both constructs was observed at day 1 and with a very similar response profile also after 24 additional hours of starvation in FCS cell culture medium at day 2 (Fig. 8). However, absolute values of luciferase induction by TGF-β_1 were higher at day 1 when compared with day 2. These results demonstrate that the time-point of the analysis has to be defined to determine the characteristic dynamic behaviour of signal transduction pathways in primary hepatocytes.

3.6 HGF induces phosphorylation of AKT/PKB and ERK1/2

Stimulation of hepatocytes with HGF leads to the activation of the PI3-kinase and MAP-kinase signalling cascades. A central component of the PI3-kinase signalling pathway is the serine/threonine kinase Akt. ERK1/2 represent central members of the MAP-kinase cascade. To analyse, whether both signalling pathways can be efficiently activated in our *in vitro* system, hepatocytes were starved for 4 h followed by 20 min stimulation with HGF (20 ng/ml). Basal levels of both pAKT/PKB and pERK1/2 were low after starvation (Fig. 9*a*). HGF caused a strong increase in pAKT/PKB and pERK1/2, whereas the levels of total AKT/PKB and ERK2 protein remained unaltered (Fig. 9*a*). Thus, the activation of PI3K-Akt and ERK signalling pathways can be reliably quantified in our *in vitro* system. Using similar conditions also insulin caused a strong phosphorylation of ERK1/2 (Fig. 9*b*).

3.7 Dynamic time-dependent NF-κB DNA-binding after TNF-α stimulation

Another signalling pathway activated during hepatocyte regeneration is the NF-κB signalling cascade. To study this pathway in our *in vitro* system, culture conditions for the hepatocytes had to be established that ensure low basal levels of NF-κB DNA-binding activity but high levels after TNF-α stimulation. To monitor NF-κB DNA-binding activity EMAs were performed. For

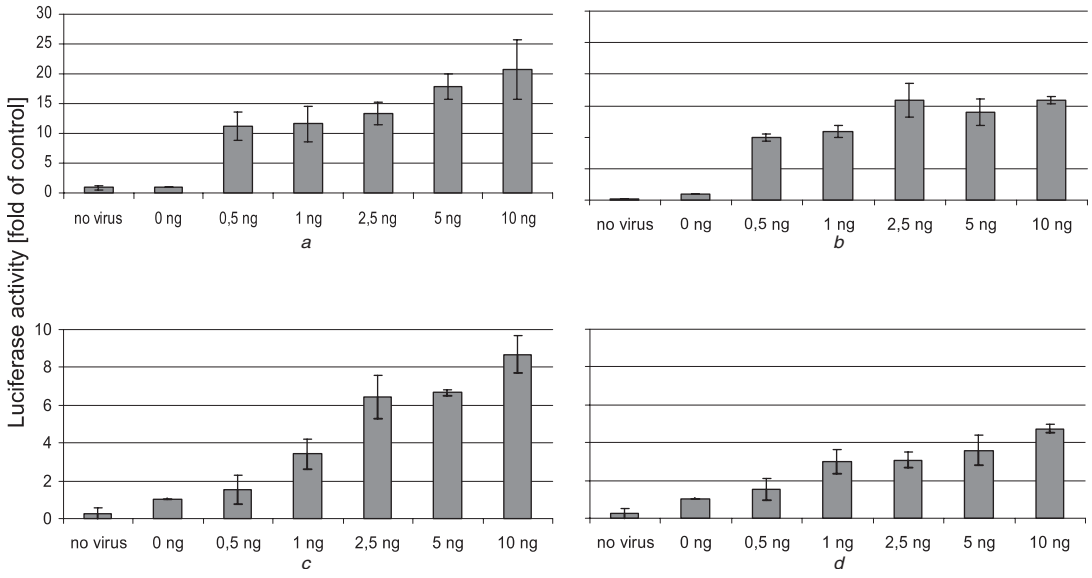

Fig. 8 *TGF-β reporter gene assays in primary mouse hepatocytes after culture periods of 1 and 2 days in FCS cell culture medium*

Luciferase expression is controlled by SMAD3/4 ('CAGA-Luc') or SMAD1/5 ('BRE-Luc') responsive motifs, respectively, that were adenovirally delivered to the cells
Hepatocytes were either infected with viruses directly after the attachment phase (4 h) followed by serum starvation overnight and TGF-β stimulation (4 h) on the next day (day 1) or the cells were infected on day 1 and stimulated on day 2 as described in Fig. 5
One representative experiment using the same cell preparation for both time-points is shown and the average values of triplicates $\pm$SD normalised to the corresponding untreated controls are presented
a CAGA-Luc, day1
b CAGA-Luc, day2
c BRE-Luc, day1
d BRE-Luc, day2

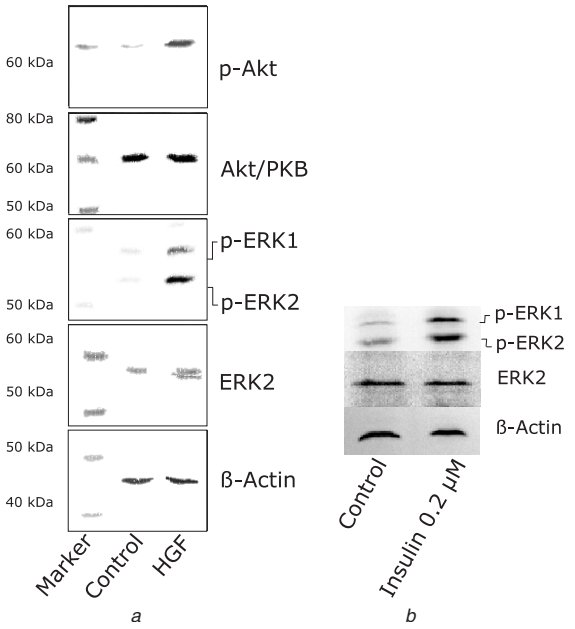

Fig. 9 *Phosphorylation of Akt/PKB and ERK1/2 after stimulation HGF*

a After 16 h in pre-starvation and 4 h in BSA-free starvation medium hepatocytes were incubated with 20 ng/ml HGF for 20 min
HGF caused a clear increase in phosphorylated Akt/PKB (p-Akt) and phosphorylated ERK1/2 (p-ERK1/2), whereas expression of the total protein (Akt, ERK1/2) remained unaltered. β-actin was used as a loading control
b Using the same conditions hepatocytes were incubated with 0.2 µM insulin for 20 min resulting in an increase of phosphorylated ERK1/2 (p-ERK1/2)

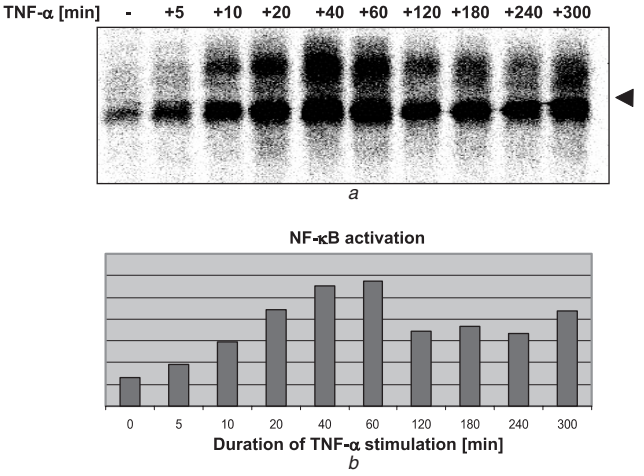

Fig. 10 *Dynamic time-dependent NF-κB DNA-binding after different periods of TNF-α stimulation*

After 2 h in serum-free cell culture medium, hepatocytes were washed with PBS, incubated in starvation medium for 24 h and stimulated with 1 ng/ml TNF-α
Subsequently, nuclear extracts were prepared. Extracts from cells without stimulation were used as controls
Equal amounts of protein from nuclear extracts were incubated with ^{33}P-labelled oligonucleotides as a probe and analysed for NF-κB activity by EMSA
a Filled arrowhead indicates the position of NF-κB oligonucleotide complexes
b NF-κB binding activities were quantified by EMSA using a phosphoImager

unstimulated hepatocytes cultured in serum-free culture medium, NF-κB DNA-binding activity decreased between day 1 and 4 reaching very low levels at day 4 (data not shown). A more rapid decrease was achieved by starvation of the hepatocytes and the best results were obtained by starvation for 24 h. Addition of BSA to the starvation medium did not accelerate the decrease in NF-κB, DNA-binding activity (data not shown). To investigate the dynamic activation of NF-κB, a time-course using different time intervals (5, 10, 20, 40, 60, 120, 180, 240 and 300 min) of TNF-α stimulation was performed. Hepatocytes incubated in starvation medium for 24 h were stimulated with TNF-α subsequently used for the preparation of nuclear extracts and studied in EMSAs. An increase in NF-κB DNA-binding activity was observed during the first 60 min (Fig. 10). Subsequently, NF-κB DNA-binding activity decreased, but levels still remained above the controls up to the longest incubation period tested (300 min). In competition assays and antibody-based analysis, including supershift and immunoblot analysis, we identified that the formed complex consists of an NF-κB p52/p65 heterodimer. Thus, TNF-α stimulation of starved hepatocytes leads to dynamic, time-dependent NF-κB activation.

3.8 Activation of β-catenin signalling

Degradation of β-catenin by the ubiquitin/proteasome pathway requires its prior phosphorylation by GSK3β [40, 41]. Abrogating β-catenin phosphorylation by Wnt growth factors or chemical inhibitors of GSK3β, leads to the accumulation of hypophosphorylated, uncomplexed β-catenin in the cytosol [41, 42]. This signalling-competent free cytosolic fraction of β-catenin can be analysed by affinity precipitation using a GST fusion protein containing the cytoplasmic tail of E-cadherin, a high-affinity binding partner of β-catenin (GST–ECT fishing; [42]). We used this method to analyse whether β-catenin signalling can be activated in our *in vitro* system. Primary mouse hepatocytes were isolated according to standard procedures, starved and then treated with the GSK3β inhibitor SB216763 [43] for increasing periods of time. Upon preparation of whole cellular lysates and GST–ECT fishing, β-catenin which could be recovered by affinity precipitation, was analysed by quantitative immunoblotting. Whereas lysates from control cells contain only little β-catenin available for affinity precipitation, free cytosolic β-catenin starts to accumulate within 1 h in cells stimulated with SB216763 (Fig. 11*a*, top). Quantitative analyses revealed that the free pool of β-catenin is increased up to approximately 27-fold over levels in unstimulated cells and reaches a plateau 6 h after blocking GSK3β (Fig. 11*b*). In contrast to the observed surge of the free cytosolic pool, total amounts of β-catenin in SB216763-treated cells remained constant (Fig. 11*a*, bottom). This is because the antibody used simultaneously recognises pre-existing β-catenin, for example engaged in cadherin-mediated cell–cell adhesion, and the population which gradually builds up in the presence of the GSK3β inhibitor. Apparently, the vast majority of β-catenin present in hepatocytes is incorporated into cadherin–catenin complexes, which remain unaffected by the activation of β-catenin signalling [41, 42]. Yet, our experiments demonstrate that a signalling-competent pool of β-catenin can be induced in primary mouse hepatocytes in time-dependent manner.

3.9 FasL treatment leads to apoptotic cell death

Injection of FasL or anti-Fas antibodies into the liver results in fulminant liver apoptosis which primarily affects

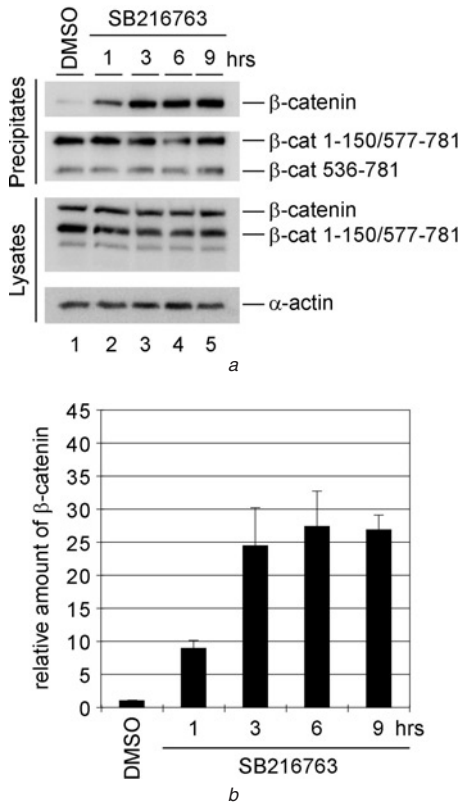

Fig. 11 *Induction of a signalling-competent pool of free cytosolic β-catenin in primary mouse hepatocytes*

a To induce a free cytosolic pool of β-catenin, 5×10^6 primary mouse hepatocytes, seeded in collagen-coated 10 cm dishes, were kept in starvation medium for 16 h and then treated with 80 μM SB216763 for the indicated periods of time (lanes 2–5)
Controls received a corresponding volume of DMSO (lane 1)
Cells were harvested and cell lysates were prepared. To recover the pool of free cytosolic β-catenin, samples of each cell lysate were supplemented with glutathione sepharose beads and the GST–ECT fusion protein
To monitor the efficacy of GST–ECT recovery, a GST–β-catenin calibrator protein was additionally added (β-cat 1–150/577–781)
After the binding reaction and extensive washing, proteins bound to the glutathione sepharose matrix were eluted with SDS–PAGE loading buffer
An additional GST–β-catenin calibrator (β-cat 536–781) was added to each sample before the final protein mixtures were separated by SDS–PAGE and analysed by immunoblotting with an antibody simultaneously recognising cellular β-catenin and the GST–β-catenin calibrator proteins. In parallel, a sample of each lysate used for the GST–ECT fishing assay was combined with the two GST–β-catenin calibrator proteins and analysed by immunoblotting with anti-β-catenin and anti-actin antibodies
b Chemiluminescent reactions from GST–ECT fishing experiments as described in *a* were recorded with the LumiImager and were analysed by the LumiAnalyst Software
Results shown are average values from three independent experiments Standard deviations are indicated. Levels of β-catenin precipitated from lysates of cells stimulated with SB216763 for different periods of time are expressed as relative amounts compared to those derived from DMSO-treated cells (the latter were arbitrarily assigned a value of one)

hepatocytes [44]. We analysed whether in our *in vitro* system, the hepatocytes retained sensitivity to undergo apoptosis in response to this death agent. As shown in Fig. 12*a* incubation of the hepatocytes with FasL from conditioned medium of FasL-producing Neuro-2a cells for 1 h provoked typical features of hepatocyte apoptosis such as cell surface exposure of phosphatidylserine as determined by annexin-V-GFP staining and absence of PI staining. After 6 h of incubation in FasL, late stages of apoptosis such as cell shrinkage, membrane blebbing and severe nuclear fragmentation were evident in the hepatocytes. To substantiate our observations, we performed DNA-laddering experiments. In line with the microscopic studies after 1 h of FasL treatment, DNA-laddering is initiated and severely present after 6 h of incubation in FasL indicative for late stages of apoptosis (Fig. 12*b*). These findings set the stage to reproducibly measure components of FasL-induced signalling in hepatocytes.

3.10 Time-course of STAT3 activation after IL-6 stimulation

To validate our SOPs, we monitored the activation of STAT3. Cells of two mice were kept in starvation medium for 5 h and subsequently stimulated with IL-6 (40 ng/ml). A total number of 2×10^6 cells per time-point were lysed and STAT3 was precipitated from the lysate. By loading time-points alternating on more than one gel, the number of data points was increased beyond gel capacity (Fig. 13*a*). Employing error reduction methods [28] enabled the generation of high resolved time-course data. The high resolution and low dispersion of the data points allowed a smoothing of the data by splines (Fig. 13*b*).

4 Discussion

Mathematical modelling of signal transduction pathways in mammalian cells requires a standardized *in vitro* system that allows rapid and reproducible generation of data. In addition, culture conditions should be as simple as reasonably possible. Here, we established and validated an *in vitro* system with primary mouse hepatocytes that fulfils the necessary criteria to permit analysis by a systems biology approach.

Ideally, an *in vitro* system for analysis of signal transduction should ensure low basal activities but high responsiveness to specific stimuli. In this aspect, the requirements for signal transduction studies differ from those needed for instance in drug metabolism studies. For the latter, cultured hepatocytes should show metabolic activities similar to the *in vivo* situation [13, 45, 46]. Different conditions are required for studies of signal transduction, since an *in vivo*-like simultaneous activation of several signalling pathways is problematic and would hinder quantification of kinetic constants, at least during an initial phase of modelling. To achieve the required low basal activities, hepatocytes have to be 'starved' in serum-free culture medium. Obviously, starving in the absence of serum and hormonal additives is unphysiological and may cause stress to starved cells [47]. If stress exceeds a certain limit, it may compromise hepatocellular functions including signal transduction. To minimise starving-associated stress, we established a three-step starving procedure (Fig. 1). During a first step, the culture medium contains FCS (10%) and dexamethasone (100 nM) to allow an efficient attachment of hepatocytes to collagen-coated dishes. After an attachment period of 4 h, the FCS cell culture medium is replaced by a serum-free cell culture medium for a 14–20 h (overnight) 'pre-starvation' period. During pre-starvation, the serum-free culture medium still contains a low concentration of dexamethasone (100 nM), as the latter is crucial for hepatocyte physiology [14, 15, 47]. 'Pre-starvation' is followed by 2–8 h of 'full starvation', where the culture medium is free of additives except antibiotics and 2 mM L-glutamine. The period of 'full starvation' depends on the time required to allow a decrease in basal activities to zero or almost zero, whereby usually 4–5 h are sufficient. An exception was NF-κB DNA-binding, requiring a starvation period of 24 h. Therefore depending on the specific signal transduction pathway, slight modifications regarding the third step

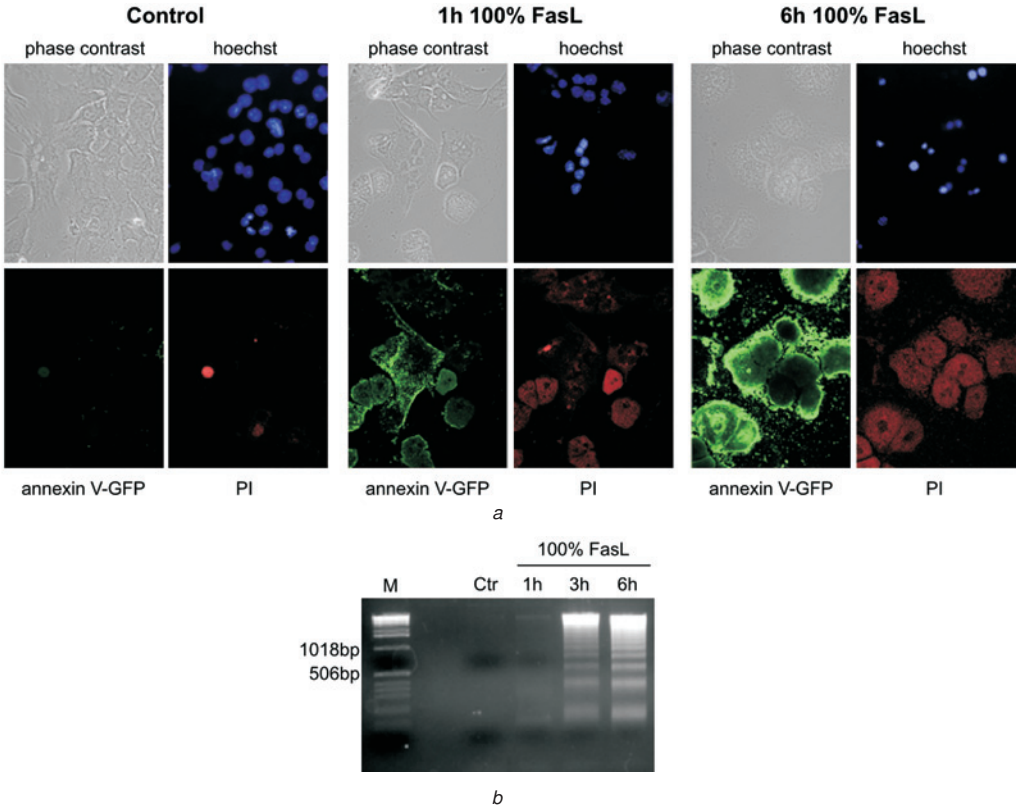

Fig. 12 *Apoptotic features of primary mouse hepatocytes*

Cells were starved for 12 h and treated with conditioned medium of FasL-expressing Neuro-2a cells for 1, 3 and 6 h or left untreated
a Phase contrast pictures show detachment, shrinkage and membrane blebbing of the cells
The hoechst stain displays disintegration of the nuclei. Extracellular phosphatidyl-serine exposure in the plasma membrane was measured by annexin-V-GFP binding (green) and PI incubation
Red staining indicates permeability of cell membranes, staining late apoptotic (cytosolic staining) and necrotic (cytosolic and nuclear staining) cells
b Analysis of the apoptotic state of FasL-treated cells by DNA-laddering
DNA was isolated from RIPA lysates by chlorofom–phenol extraction
The DNA was separated on a 1.7% agarose gel indicating beginning of DNA fragmentation after 1 h with increasing intensity at 3 and 6 h, whereas untreated cells (ctr) do not show fragmentation of the DNA

of the starving procedure are necessary to reduce basal signal transduction activity.

Liver cell fractions isolated by collagenase perfusion usually contain approximately 98% hepatocytes, the main functional cells of the liver, and 2% non-parenchymal cells, including (i) biliary epithelial cells (lining biliary ducts); (ii) fenestrated endothelial cells, representing a unique type of endothelial cells with large cytoplasmic gaps (fenestrae) that allow maximal contact between circulating blood and hepatocytes; (iii) Kupffer cells, which are macrophages in hepatic sinusoids; and (iv) hepatic stellate cells, a cell type located in the space of disse between hepatocytes and endothelial lining cells, with several functions, for example storage of vitamin A, synthesis of connective tissue and secretion of several growth factors after activation by liver damage and during fibrogenesis [19, 20]. In agreement with the previous studies [11, 48], we observed a strong reduction of the non-parenchymal cell fraction after Percoll centrifugation. However, a disadvantage of this technique is the high loss of hepatocyte numbers. Usually, immunoblot-based experiments can be performed without this additional purification step because of the relatively small fraction of protein contributed by the non-parenchymal cell fraction. RT–PCR analysis may be more problematic. Another complication may be the release of cytokines from non-parenchymal cells leading to secondary effects in hepatocytes. For instance, TNF-α has been reported to stimulate IL-6 secretion by Kupffer cells [19, 20]. Usually, secondary effects will not compromise analysis of signalling in hepatocytes, if short analytical periods are used. Nevertheless, a control experiment including Percoll-purified hepatocytes is recommended for each type of stimulation, before large number of experiments are performed with non-purified cell fractions.

To evaluate the extent of starving-associated stress, several metabolic functions of cultured primary hepatocytes were quantified. No major differences in activities were observed between hepatocytes cultured in FCS cell culture or in starvation medium during a serum-free culture period of 8 h. Compared with freshly isolated hepatocytes, activities decreased during the first 1–2 days in culture and later reached a new plateau. This decrease occurred independent of starvation and was similar in cell culture medium with and without FCS. Decrease in drug-metabolising activities in cultured primary hepatocytes during the initial culture period is a well-known phenomenon. Relatively complex culture conditions are required to maintain high-metabolising activities of freshly isolated hepatocytes, including three-dimensional culture systems and hormonal additives [13, 14, 49]. However, the latter would compromise signal transduction analysis and should be avoided in an initial phase of modelling. Establishment of constant activities after an initial decrease shows that cultured hepatocytes achieve a new equilibrium state, even in the absence of stimulating factors that are present *in vivo*. Continuous withdrawal of FCS for several days results in hepatocellular decompensation. However,

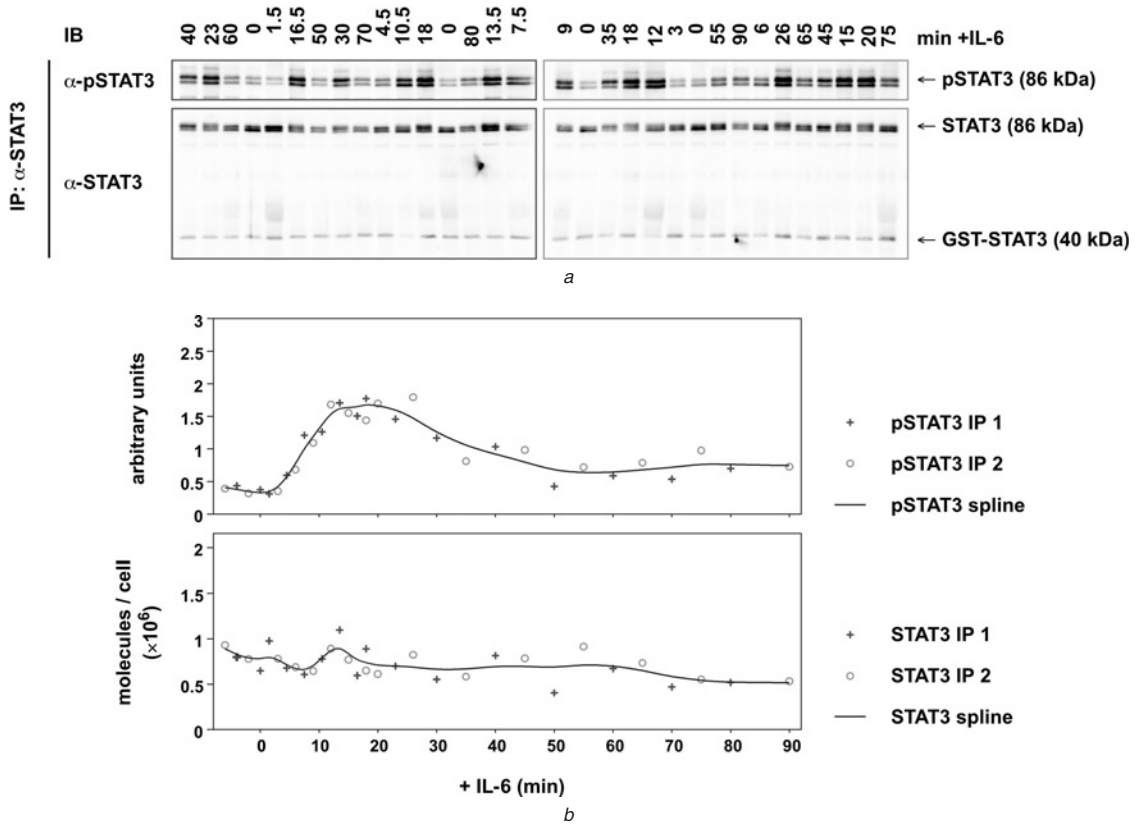

Fig. 13 *Time course of STAT3 activation upon IL-6 stimulation*

a Primary mouse hepatocytes were prepared from a pool of two mouse livers
2×10^6 cells for each time-point were cultivated on collagen-coated dishes and starved for 5 h. IL-6 (40 ng/ml) was added and the cells were lysed at the indicated time-points
STAT3 molecules were precipitated from the lysate using an αSTAT3 antibody and separated on two 10% SDS-PAGE gels
Sample loading was randomised with every second time-point on the second gel
Quantitative immunoblotting was performed with α-phospho (Y705) STAT3 and αSTAT3 antibodies
b Immunoprecipitation data was calibrated with GST–STAT3 and converted to molecules per cell for STAT3, the data points were spline-smoothed as indicated by solid lines

the relatively short starving period and performance of assays on day 1 of hepatocyte culture as presented in Fig. 1 guarantees functionality of all studied signal transduction pathways.

Using the abovementioned starving procedure (Fig. 1), we analysed responsiveness of several signal transduction pathways in hepatocytes known to be functional *in vivo*. We demonstrate a dose-dependent, reproducible and dynamic activation of the JAK–STAT, SMAD, PI3K-Akt, ras-ERK, Wnt/β-catenin and the FasL-induced signalling pathways. Phosphorylation of gp130, JAK1 and STAT3 were induced by IL6, whereas TGFβ was able to trigger the phosphorylation of SMAD1, SMAD2 and SMAD3. Both Akt/PKB and ERK1/2 were phosphorylated after stimulation with HGF. A signalling competent pool of β-catenin was detected after inhibition of GSK3β mimicking ligand-induced activation of the Wnt/β-catenin signalling pathway. To analyse, whether phosphorylation is actually leading to transcriptional responses, a luciferase reporter gene driven by multiple copies of a TGF-β response motif was applied, demonstrating a dose-dependent increase in luciferase activity.

Culture conditions in the present study were chosen to guarantee low basal activities of signal transduction pathways. Therefore we avoided hormonal additives to the starving media. In contrast, culture media free of serum and hormonal additives are not optimal for long-term maintenance of primary hepatocytes. Experiments with reporter constructs including a SMAD3/4 and a SMAD1/5 luciferase construct demonstrated a qualitatively similar response to TGF-β_1, but the extent of luciferase induction was slightly lower if hepatocytes were cultured for additional 24 h. Therefore using our conditions we recommend performing all analyses for modelling of signal transduction in primary mouse hepatocytes at day 1. If longer culture periods are required, more complex conditions are needed, for instance as described by Block *et al.* [14]. Nevertheless, analysis at day 1 usually will be sufficient for generation of data for modelling, as relatively short analytical periods of 1–4 h after stimulation are sufficient. Under these conditions, apoptotic signalling can also be studied. In response to FasL apoptosis was triggered in a time-dependent manner, as expected from previous reports [50]. In conclusion, all of the studied signal transduction pathways were active in our mouse hepatocyte *in vitro* system including a three-step starving procedure. This will permit the generation of high-quality quantitative data for mathematical modelling of signalling pathways as shown for the activation of STAT3 (Fig. 6).

5 Acknowledgment

This study was supported by the German Federal Ministry of Education and Research (BMBF), funding priority HepatoSys 'Systems of Life–Systems Biology'. The authors would like to thank Dr. Gisela Miczka and Dr. Erich Stüttgen, Projektträger Jülich, for excellent organisation of our research network and Dr. Ute Heisner for excellent project management. We also thank A. Fontana for providing us with the FasL-expressing Neuro-2a cell line.

6 References

1 Swameye, I., Müller, T.G., Timmer, J., Sandra, O., and Klingmüller, U.: 'Identification of nucleocytoplasmic cycling as a remote sensor in cellular signalling by databased modelling', *Proc. Natl Acad. Sci. USA*, 2003, **100**, pp. 1028–1033

2 Hoffmann, A., Levchenko, A., Scott, M.L., and Baltimore, D.: 'The IkappaB-NF-kappaB signaling module: temporal control and selective gene activation', *Science*, 2002, **298**, pp. 1241–1245

3 Bentele, M., Lavrik, I., Ulrich, M., Stosser, S., Heermann, D.W., Kalthoff, H., Krammer, P.H., and Eils, R.: 'Mathematical modeling reveals threshold mechanism in CD95-induced apoptosis', *J. Cell Biol.*, 2004, **166**, pp. 839–851

4 Hengstler, J.G., Brulport, M., Schormann, W., Bauer, A., Hermes, M., Nussler, A., Fandrich, F., Ruhnke, M., Ungefroren, H., Griffin, L., Bockamp, E.O., Oesch, F., and von Mach, M.A.: 'Generation of human hepatocytes by stem cell technology: definition of the hepatocyte', *Exp. Opin. Drug Metab. Toxicol.*, 2006, **1**, pp. 61–74

5 Beerheide, W., von Mach, M.A., Ringel, M., Fleckenstein, C., Schumann, S., Renzing, N., Hildebrandt, A., Brenner, W., Jensen, O., Gebhard, S., Reifenberg, K., Bender, J., Oesch, F., and Hengstler, J.G.: 'Downregulation of beta2-microglobulin in human cord blood somatic stem cells after transplantation into livers of SCID-mice: an escape mechanism of stem cells?', *Biochem. Biophys. Res. Commun.*, 2002, **294**, pp. 1052–1063

6 von Mach, M.A., Hengstler, J.G., Brulport, M., Eberhardt, M., Schormann, W., Hermes, M., Prawitt, D., Zabel, B., Grosche, J., Reichenbach, A., Muller, B., Weilemann, L.S., and Zulewski, H.: '*In vitro* cultured islet-derived progenitor cells of human origin express human albumin in severe combined immunodeficiency mouse liver *in vivo*', *Stem Cells*, 2004, **22**, pp. 1134–1141

7 Ruhnke, M., Ungefroren, H., Nussler, A., Martin, F., Brulport, M., Schormann, W., Hengstler, J.G., Klapper, W., Ulrichs, K., Hutchinson, J.A., Soria, B., Parwaresch, R.M., Heeckt, P., Kremer, B., and Fändrich, F.: 'Reprogramming of human peripheral blood monocytes into functional hepatocyte and pancreatic islet-like cells', *Gastroenterology*, 2005, **128**, pp. 1774–1786

8 Steinberg, P., Fischer, T., Kiulies, S., Biefang, K., Platt, K.-L., Oesch, F., Böttger, Th., Bulitta, C., Kempf, P., and Hengstler, J.G.: 'Drug metabolizing capacity of cryopreserved human, rat and mouse liver parenchymal cells in suspension', *Drug Metab. Dispos.*, 1999, **27**, pp. 1415–1422

9 Li, A.P., Gorycki, P.D., Hengstler, J.G., Kedderis, G.L., Koebe, H.G., Rahmani, R., de Sousas, G., Silva, J.M., and Skett, P.: 'Present status of the application of cryopreserved hepatocytes in the evaluation of xenobiotics: consensus of an international expert panel', *Chem. Biol. Interact.*, 1999, **121**, pp. 117–123

10 Hengstler, J.G., Ringel, M., Biefang, K., Hammel, S., Milbert, U., Gerl, M., Klebach, M., Diener, B., Platt, K.L., Böttger, T., Steinberg, P., and Oesch, F.: 'Cultures with cryopreserved hepatocytes: applicability for studies of enzyme induction', *Chemico Biol. Interact.*, 2000a, **125**, pp. 51–73

11 Hengstler, J.G., Utesch, D., Steinberg, P., Ringel, M., Swales, N., Biefang, K., Platt, K.L., Diener, B., Böttger, T., Fischer, T., and Oesch, F.: 'Cryopreserved primary hepatocytes as an *in vitro* model for the evaluation of drug metabolism and enzyme induction', *Drug Metab. Rev.*, 2000b, **32**, pp. 81–118

12 Hengstler, J.G., Bogdanffy, M.S., Bolt, H.M., and Oesch, F.: 'Challenging dogma: thresholds for genotoxic carcinogens? The case of Vinyl Acetate', *Annu. Rev. Pharmacol. Toxicol.*, 2003, **43**, pp. 485–520

13 Gebhardt, R., Hengstler, J.G., Müller, D., Glöckner, R., Buenning, P., Laube, B., Schmelzer, E., Ullrich, M., Utesch, D., Hewitt, N., Ringel, M., Reder Hilz, B., Bader, A., Langsch, A., Koose, T., Burger, H.J., Maas, J., and Oesch, F.: 'New hepatocyte *in vitro* systems for drug metabolism: metabolic capacity and recommendations for application in basic research and drug development, standard operation procedures', *Drug Metab. Rev.*, 2003, **35**, pp. 145–213

14 Block, G.D., Locker, J., Bowen, W.C., Petersen, B.E., Katyal, S., Strom, S.C., Riley, T., Howard, T.A., and Michalopoulos, G.K.: 'Population expansion, clonal growth, and specific differentiation patterns in primary cultures of hepatocytes induced by HGF/SF, EGF and TGF alpha in a chemically defined (HGM) medium', *J. Cell Biol.*, 1996, **132**, pp. 1133–1149

15 Ringel, M., Oesch, F., Bader, A., Gerl, M., Klebach, M., Quint, M., Tanner, B., Dillenburg, W., Böttger, T., and Hengstler, J.G.: 'Permissive and suppressive effects of dexamethasone on enzyme induction in hepatocyte cultures', *Xenobiotica*, 2002, **32**, pp. 653–666

16 Ringel, M., von Mach, M.A., Santos, R., Feilen, P.J., Brulport, M., Hermes, M., Bauer, A.W., Schormann, W., Tanner, B., Schon, M.R., Oesch, F., and Hengstler, J.G.: 'Hepatocytes cultured in alginate microspheres: an optimized technique to study enzyme induction', *Toxicology*, 2005, **206**, pp. 153–167

17 Osterod, M., Hollenbach, S., Hengstler, J.G., Barnes, D.E., Lindahl, T., and Epe, B.: 'Age-related and tissue-specific accumulation of oxidative DNA base damage in 7,8-dihydro-8-oxoguanine-DNA glycosylase (*ogg1*) deficient mice', *Carcinogenesis*, 2001, **22**, pp. 1459–1463

18 Osterod, M., Larsen, E., Le Page, F., Hengstler, J.G., Van Der Horst, G.T., Boiteux, S., Klungland, A., and Epe, B.: 'A global DNA repair mechanism involving the Cockayne syndrome B (CSB) gene product can prevent the *in vivo* accumulation of endogenous oxidative DNA base damage', *Oncogene*, 2002, **28**, pp. 8232–8239

19 Michalopoulos, G.K., and DeFrances, M.C.: 'Liver regeneration', *Science*, 1997, **276**, pp. 60–66

20 Michalopoulos, G.K., and DeFrances, M.: 'Liver regeneration', *Adv. Biochem. Eng. Biotechnol.*, 2005, **93**, pp. 101–134

21 Michalopoulos, G.K., Barua, L., and Bowen, W.C.: 'Transdifferentiation of rat hepatocytes into biliary cells after bile duct ligation and toxic biliary injury', *Hepatology*, 2005, **41**, pp. 535–544

22 Schwabe, R.F., Uchinami, H., Qian, T., Bennett, B.L., Lemasters, J.J., and Brenner, D.A.: 'Differential requirement for c-Jun NH2-terminal kinase in TNFalpha- and Fas-mediated apoptosis in hepatocytes', *FASEB J.*, 2004, **18**, (6), pp. 720–722

23 Kruithof-de Julio, M., Labruyere, W.T., Ruijter, J.M., Vermeulen, J.L., Stanulovic, V., Stallen, J.M., Baldysiak-Figiel, A., Gebhardt, R., Lamers, W.H., and Hakvoort, T.B.: 'The RL-ET-14 cell line mediates expression of glutamine synthetase through the upstream enhancer/promoter region', *J. Hepatol.*, 2005, **43**, (1), pp. 126–131

24 Reder-Hilz, B., Ullrich, M., Ringel, M., Hewitt, N., Utesch, D., Oesch, F., and Hengstler, J.G.: 'Metabolism of propafenone and verapamil by cryopreserved human, rat mouse and dog hepatocytes: comparison with metabolism *in vivo*', *Naunyn Schmiedebergs Arch. Pharmacol.*, 2004, **369**, pp. 408–417

25 Carmo, H., Hengstler, J.G., de Boer, D., Ringel, M., Carvalho, F., Fernandes, E., Remiao, F., dos Reys, L.A., Oesch, F., and de Lourdes Bastos, M.: 'Comparative metabolism of the designer drug 4-methylthioamphetamine by hepatocytes from man, monkey, dog, rabbit, rat and mouse', *Naunyn Schmiedebergs Arch. Pharmacol.*, 2004, **369**, pp. 198–205

26 Shimizu, M., Fontana, A., Takeda, Y., Yagita, H., Yoshimoto, T., and Matsuzawa, A.: 'Induction of antitumor immunity with Fas/APO-1 ligans (CD95L)-transfected neuroblastoma Neuro-2a cells', *J. Immunol.*, 1999, **162**, pp. 7350–7357

27 Schilling, M., Maiwald, T., Bohl, S., Kollmann, M., Kreutz, C., Timmer, J., and Klingmuller, U.: 'Computational processing and error reduction strategies for standardized quantitative data in biological networks', *FEBS J.*, 2005, **272**, (24), pp. 6400–6411

28 Schiffer, I.B., Gebhard, S., Heimerdinger, C.K., Heling, A., Hast, J., Wollscheid, U., Seliger, B., Tanner, B., Gilbert, S., Beckers, T., Baasner, S., Brenner, W., Spangenberg, C., Prawitt, D., Trost, T., Schreiber, W.G., Zabel, B., Thelen, M., Lehr, H.A., Oesch, F., and Hengstler, J.G.: 'Switching off her-2/neu in a tetracycline-controlled mouse tumor model leads to apoptosis and tumor-size-dependent remission', *Cancer Res.*, 2003, **63**, pp. 7221–7231

29 Trost, T.M., Lausch, E.U., Fees, S.A., Schmitt, S., Enklaar, T., Reutzel, D., Brixel, L.R., Schmidtke, P., Maringer, M., Schiffer, I.B., Heimerdinger, C.K., Hengstler, J.G., Fritz, G., Bockamp, E.O., Prawitt, D., Zabel, B.U., and Spangenberg, C.: 'Premature senescence is a primary fail-safe mechanism of ERBB2-driven tumorigenesis in breast carcinoma cells', *Cancer Res.*, 2005, **65**, pp. 840–849

30 Eger, K., Hermes, M., Uhlemann, K., Rodewald, S., Ortwein, J., Brulport, M., Bauer, A., Schormann, W., Lupatsch, F., Schiffer, I., Heimerdinger, C., Gebhard, S., Spangenberg, C., Pravitt, D., Trost, T., Zabel, B., Tanner, B., Krugel, U., Franke, H., Illes, P., Madaj-Sterba, P., Bockamp, E.O., Beckers, T., and Hengstler, J.G.: '4-Epidoxycycline: an alternative to doxycycline to control gene expression in conditional mouse models', *Biochem. Biophys. Res. Commun.*, 2004, **323**, pp. 979–986

31 Micke, P., Hengstler, J.G., Ros, R., Bittinger, F., Metz, T., Gebhard, S., Beeh, K.M., Oesch, F., and Buhl, R.: 'C-erbB-2 expression in small cell lung cancer is associated with poor prognosis', *Int. J. Cancer*, 2001, **92**, pp. 474–479

32 Micke, P., Basrai, M., Faldum, A., Bittinger, F., Ronnstrand, L., Blaukat, A., Beeh, K.M., Oesch, F., Fischer, B., Buhl, R., and Hengstler, J.G.: 'Characterization of c-kit expression in small cell lung cancer: prognostic and therapeutic implications', *Clin. Cancer Res.*, 2003, **9**, pp. 188–194

33 Aberle, H., Bauer, A., Stappert, J., Kispert, A., and Kemler, R.: 'beta-Catenin is a target for the ubiquitin-proteasome pathway', *EMBO J.*, 1997, **16**, pp. 3797–3804

34 Hecht, A., Litterst, C.M., Huber, O., and Kemler, R.: 'Functional characterization of multiple transactivating elements in beta-catenin, some of which interact with the TATA-binding protein *in vitro*', *J. Biol. Chem.*, 1999, **274**, pp. 18017–18025

35 Korchynskyi, O., and ten Dijke, P.: 'Identification and functional characterization of distinct critically important bone morphogenetic protein-specific response elements in the Id1 promoter', *J. Biol. Chem.*, 2002, **77**, pp. 4883–4891
36 Egger, L., Schneider, J., Rheme, C., Tapernoux, M., Häcki, J., and Borner, C.: 'Serine proteases mediate apoptosis-like cell death and phagocytosis under caspase-inhibiting conditions', *Cell Death Differ.*, 2003, **10**, pp. 1188–1203
37 Levintow, L.: 'The glutamyltransferase activity of normal and neoplastic tissues', *J. Natl. Cancer.*, 1954, **15**, pp. 347–352
38 Gebhardt, R., and Williams, G.M.: 'Amino acid transport in established adult rat liver epithelial cell lines', *Cell Biol. Toxicol.*, 1986, **2**, pp. 9–20
39 Westhoff, J.H., Sawitza, I., Keski-Oja, J., Gressner, A.M., and Breitkopf, K.: 'PDGF-BB induces expression of LTBP-1 but not TGF-beta1 in a rat cirrhotic fat storing cell line', *Growth Factors*, 2003, **21**, pp. 121–130
40 van Noort, M., Meeldijk, J., van der Zee, R., Destree, O., and Clevers, H.: 'Wnt signaling controls the phosphorylation status of beta-catenin', *J. Biol. Chem.*, 1999, **277**, pp. 17901–17905
41 Wodarz, A., and Nusse, R.P.: 'Mechanisms of Wnt signaling in development', *Annu. Rev. Cell Dev. Biol.*, 1998, **14**, pp. 59–88
42 Aberle, H., Schwartz, H., Hoschuetzky, H., and Kemler, R.: 'Single amino acid substitutions in proteins of the armadillo gene family abolish their binding to alpha-catenin', *J. Biol. Chem.*, 1996, **271**, pp. 1520–1526
43 Coghlan, M.P., Culbert, A.A., Cross, D.A., Corcoran, S.L., Yates, J.W., Pearce, N.J., Rausch, O.L., Murphy, G.J., Carter, P.S., and Roxbee Cox, L., *et al.*: 'Selective small molecule inhibitors of glycogen synthase kinase-3 modulate glycogen metabolism and gene transcription', *Chem. Biol.*, 2000, **7**, pp. 793–803
44 Ogasawara, J., Watanabe-Fukunaga, R., Adachi, M., Matsuzawa, A., Kasugai, T., Kitamura, Y., Itoh, N., Suda, T., and Nagata, S.: 'Lethal effect of the anti-fas antibody in mice', *Nature*, 1993, **364**, pp. 806–809
45 Carmo, H., Hengstler, J.G., Boer, D., Ringel, M., Remiao, F., Carvalho, F., Fernandes, E., Reys, L.A., Oesch, F., and Bastos Mde, L.: 'Metabolic pathways of 4-bromo-2,5-dimethoxyphenethylamine (2C-B): analysis of phase I metabolism with hepatocytes of six species including human', *Toxicology*, 2005, **206**, pp. 75–89
46 Arand, M., Herrero Plana, M.E., Hengstler, J.G., Lohmann, M., Cronin, A., and Oesch, F.: 'Detoxification strategy of epoxide hydrolase the basis for a threshold in chemical carcinogenesis', *EXCLI J.*, 2003, **22**, pp. 22–30
47 Sidhu, J.S., Liu, F., and Omiecinski, C.J.: 'Phenobarbital responsiveness as a uniquely sensitive indicator of hepatocyte differentiation status: requirement of dexamethasone and extracellular matrix in establishing the functional integrity of cultured primary rat hepatocytes', *Exp. Cell Res.*, 2004, **292**, pp. 252–264
48 Hasmall, S.C., West, D.A., Olsen, K., and Roberts, R.A.: 'Survival and function of isolated hepatocytes after cryopreservation', *Carcinogenesis*, 2000, **21**, pp. 2159–2165
49 Runge, D., Michalopoulos, G.K., Strom, S.C., and Runge, D.M.: 'Recent advances in human hepatocyte culture systems', *Biochem. Biophys. Res. Commun.*, 2000, **274**, pp. 1–3
50 Woo, M., Hakem, A., Elia, A.J., Hakem, R., Duncan, G.S., Patterson, B.J., and Mak, T.W.: '*In vivo* evidence that caspase-3 is required for Fas-mediated apoptosis of hepatocytes', *J. Immunol.*, 1999, **163**, pp. 4909–4916